ORIGINAL ARTICLE

Human liver stem cell-derived extracellular vesicles reduce injury in a model of normothermic machine perfusion of rat livers previously exposed to a prolonged warm ischemia

Nicola De Stefano[1] (iD), Victor Navarro-Tableros[2] (iD), Dorotea Roggio[1], Alberto Calleri[1] (iD), Federica Rigo[1] (iD), Ezio David[3], Alessandro Gambella[3] (iD), Daniela Bassino[4], Antonio Amoroso[5] (iD), Damiano Patrono[1] (iD), Giovanni Camussi[6] (iD) & Renato Romagnoli[1] (iD)

1 General Surgery 2U, Liver Transplantation Center, AOU Città della Salute e della Scienza di Torino, University of Turin, Turin, Italy
2 2i3T - Società per la gestione dell'incubatore di imprese e per il trasferimento tecnologico dell'Università degli Studi di Torino, Scarl. - Molecular Biotechnology Center (MBC), Turin, Italy
3 Pathology Unit, Molinette Hospital, AOU Città della Salute e della Scienza di Torino, Turin, Italy
4 S.C. Banca del Sangue e Immunoematologia, AOU Città della Salute e della Scienza di Torino, Turin, Italy
5 Regional Transplantation Center, Piedmont, AOU Città della Salute e della Scienza di Torino, Turin, Italy
6 Department of Medical Sciences, University of Turin, Turin, Italy

Correspondence
Professor Renato Romagnoli, General Surgery 2U, Liver Transplantation Center, AOU Città della Salute e della Scienza di Torino, University of Turin, Corso Bramante 88-90, 10126 Torino, Italy.
Tel: 0039 011 6334374;
Fax: 0039 011 6336551;
e-mail: renato.romagnoli@unito.it

SUMMARY

Livers from donors after circulatory death (DCD) are a promising option to increase the donor pool, but their use is associated with higher complication rate and inferior graft survival. Normothermic machine perfusion (NMP) keeps the graft at 37°C, providing nutrients and oxygen supply. Human liver stem cell-derived extracellular vesicles (HLSC-EVs) are able to reduce liver injury and promote regeneration. We investigated the efficacy of a reconditioning strategy with HLSC-EVs in an experimental model of NMP. Following total hepatectomy, rat livers were divided into 4 groups: (i) healthy livers, (ii) warm ischemic livers (60 min of warm ischemia), (iii) warm ischemic livers treated with 5×10^8 HLSC-EVs/g-liver, and (iv) warm ischemic livers treated with a 25×10^8 HLSC-EVs/g-liver. NMP lasted 6 h and HLSC-EVs (Unicyte AG, Germany) were administered within the first 15 min. Compared to controls, HLSC-EV treatment significantly reduced transaminases release. Moreover, HLSC-EVs enhanced liver metabolism by promoting phosphate utilization and pH self-regulation. As compared to controls, the higher dose of HLSC-EV was associated with significantly higher bile production and lower intrahepatic resistance. Histologically, this group showed reduced necrosis and enhanced proliferation. In conclusion, HLSC-EV treatment during NMP was feasible and effective in reducing injury in a DCD model with prolonged warm ischemia.

Introduction

Liver transplantation (LT) is still burdened with a considerable discrepancy between the number of patients on the waiting list and the availability of donors. In an attempt to reduce this limitation, the use of extended criteria donor (ECD) organs has increased. ECD characteristics include advanced donor age, macro-steatosis, prolonged cold ischemia time, or donation after circulatory death (DCD). The use of DCD grafts, in particular, allowed to significantly increase the number of LT procedures, [1] but was frequently associated with worse postoperative outcomes [2,3]. However, the development of more appropriate allocation strategies and the introduction of liver perfusion machines are now changing this scenario [4,5].

The gold standard for liver preservation before LT is represented by static cold storage (SCS), which consists in the rapid cooling of the organ, slowing hepatocellular metabolism; however, this technique is less effective in protecting sub-optimal grafts from ischemia/reperfusion injury (IRI) [6]. Considering the increased vulnerability of ECD livers to ATP depletion during cold ischemia [7], a valid alternative to preserve ECD livers is represented by the ex vivo normothermic machine perfusion (NMP), a device that supplies hepatocytes with oxygen and nutrients, maintaining the organ at physiological temperature [8]. During NMP, the liver is metabolically active, as confirmed by continuous production of bile, lactate clearance, and glucose consumption [9]. The feasibility and efficacy of NMP in the clinical setting have already been established [9,10], but whether NMP alone is able to recover extremely high-risk organs is still a challenging question [11]. In turn, one of the advantages of NMP is the opportunity to treat the graft during preservation by adding therapeutic agents directly into the perfusate [12–16]. More specifically, several approaches have been explored, including liver defatting strategies, vasodilators administration, gene-silencing, and cell therapies [15]. At present, a considerable body of literature has been produced on the use of such strategies also in large animal models and in preclinical studies (i.e., discarded human livers). In particular, stem cell therapies have been effectively applied during kidney, lung, and liver perfusion, demonstrating the feasibility of the procedure and the extremely promising reconditioning opportunities related to this approach [17].

Human liver stem cells (HLSCs) are multipotent stem cells isolated from the adult liver, which express hepatic markers such as albumin, α-fetoprotein, and cytokeratins 8 and 18 [18]. Several studies demonstrated the organ-specific differentiation and the hepatoprotective and regenerative activity of HLSCs in experimental models of liver injury [18–20]. HLSCs exert their biological activity also through paracrine mechanisms. In particular, human liver stem cell-derived extracellular vesicles (HLSC-EVs) are cell-secreted vesicles able to promote recovery of injured tissues. In fact, HLSC-EVs actively participate in the communication between stem cells and adult cells through the horizontal transfer of lipids, proteins, and, above all, genetic information, effectively translated into proteins with biological activity [21–25]. Compared to stem cell-based approaches, therapies with extracellular vesicles (EVs) are more advantageous in terms of production, storage, and administration protocols and are associated with less risk of cell instability or immunogenic response. The use of EVs during solid organ perfusion has already been proposed by different groups; in particular, EVs from mesenchymal stem cells successfully reduced IRI in experimental models of lung and kidney machine perfusion [26]. Recently, in a model of hypoxic liver reconditioning by NMP, we have shown that administered HLSC-EVs were able to localize into the hepatic parenchyma within 4 h of perfusion. The livers subjected to hypoxia during NMP benefited from treatment with HLSC-EV, reducing the release of AST and LDH and showing a significant reduction in apoptosis and necrosis [27,28]. Moreover, similar protective effects on cytolysis and histology were observed in another recent work by our group, in which HLSC-EVs were systemically administered in a mouse model of partial liver IRI. In this setting, we also found that HLSC-EVs modulated the hepatic inflammatory response to IRI at a molecular level [29].

Given these preliminary results, we aimed to investigate whether a longer NMP (6 h) enriched with HLSC-EVs is able to recondition rat livers exposed to a prolonged period (60 min) of warm ischemia.

Materials and methods

Isolation, characterization, and culture of HLSCs

The HLSCs were isolated and cultured as previously described. Additional information about the protocol can be found in Panel S1 [18,29].

Isolation of HLSC-EVs

The HLSC-EVs were obtained as previously described [18,29]. Briefly, the HLSCs were starved overnight in RPMI medium deprived of FCS at 37 °C in a humidified incubator with 5% CO_2. Supernatants were

collected, centrifuged for 30 min at 3000 g, and submitted to microfiltration with 0.22-mm filters to remove cell debris and apoptotic bodies. Supernatants were then collected and ultracentrifuged at 100 000 g for 2 h at 4 °C (Beckman Coulter Optima L-90 K, Fullerton, CA, USA). EVs were collected and labeled with 1 μM of Dil dye (1,1′-Dioctadecyl-3,3,3′,3′-tetramethylindocarbocyanine perchlorate; Molecular Probes Life Technology, New York, NY, USA), then washed in PBS, and ultracentrifuged for 1 h at 4 °C [30]. The collected Dil-stained EVs were used fresh or stored at −80 °C after re-suspension in RPMI and 1% dimethyl sulfoxide (DMSO). No differences in biological activity were observed between fresh and stored EVs (data not shown). Quantification and size distribution was performed as previously described [29,31]. Briefly, the EVs diluted (1:200) in sterile saline solution were analyzed by using NanoSight LM10 (NanoSight Ltd., Minton Park, UK) with the NTA 1.4 Analytical Software as previously [29,31].

HLSC-EV characterization was performed as described in detail in reference 27. Size and concentration of EV were determined by NanoSight LM10 (NanoSight Ltd., Minton Park, UK) with the NTA 1.4 Analytical Software. Expression of surface markers was evaluated by bead-based multiplex analysis by flow cytometry (MACSPlex Exosome Kit, human, Miltenyi Biotec), showing expression of exosomal markers CD9, CD63, and CD81 and markers of the cell of origin such as CD29, CD44, CD105, and CD49e, whereas the hematopoietic (CD3, CD4, CD8, CD19, etc.), endothelial (CD31), and epithelial (CD326) markers were negative (Fig. S1). By transmission electron microscopy (JEM 1400 flash Jeol, Tokyo, Japan), HLSC-EVs showed a homogeneous pattern of nano-sized membrane vesicles.

Animals

Animal studies were performed following the protocol approved by the Ethic Committee of the Italian Institute of Health (Istituto Superiore di Sanità, N.1164/2015-PR and N.262/2019-PR) and conducted in accordance with the National Institute of Health Guide for Care and Use of Laboratory Animals. Male Wistar rats weighting 200-250 g (8-12 weeks of age) were obtained from Charles Rivers (Italy) and had access to a standard diet and to water ad libitum at our animal facility.

Surgical procedure

Rat livers were procured as previously described [27]. A brief description of the procedure can be found in Fig. S2.

NMP system

The NMP circuit included a perfusion chamber (Harvard Apparatus, Hugo Sachs Elektronik), two peristaltic pumps (Reglo, Ismatec), a hollow fiber membrane oxygenator, a bubble trap, and a reservoir. Portal pressure was constantly maintained at 12-16 mmHg through a controller (Harvard Apparatus, Hugo Sachs Elektronik) connected to the inflow pump. System temperature was set at 37°C. The circuit was filled with 150 ml of perfusion solution, consisting of i) 100 ml of phenol red-free Williams E Medium, supplemented with 100 U/mL penicillin, 100 μg/ml streptomycin, 0,292 g/l L-glutamine (all from Sigma), 1 U/ml insulin (Lilly, Italy), 1 U/ml heparin (PharmaTex, Italy), named complete Williams Medium, and ii) 50 ml of recently expired (max. 5 days) human red blood cell concentrate (Blood Component Production and Validation Center, Molinette Hospital, Turin), thus obtaining a hematocrit of 16-20% [32]. The perfusion solution was actively oxygenated with 99% oxygen (pO$_2$ > 400 mmHg) [33], and 1 mEq of bicarbonate was added to the circuit every time pH reached values inferior to 7.3.

Two infusion pumps were used to refresh nutrients and to provide bile salts to the liver during NMP. In particular, one syringe pump was filled with 10 mg/ml of taurocholic acid (Sigma-Aldrich) and run at 1 ml/h, while a second pump was filled with 30 ml of complete Williams Medium added with 3 U/ml heparin and run at 5 ml/h.

Study design

An established rat model of long warm ischemia was used to simulate a high-risk DCD condition [34–36]. After procurement, ischemic livers were placed in a temperature-controlled chamber and maintained for 60 min at 34 °C. Animals were randomly assigned to the following experimental groups: NO INJURY group ($n = 6$): healthy livers (nonischemic) exposed to minimal cold storage (34 ± 7 min) and perfused for 6 h with NMP; WI group ($n = 6$): livers exposed to 60 min of warm ischemia followed by 6 h of NMP; WI+EV1 group ($n = 6$): livers exposed to 60 min of warm ischemia, perfused for 6 h with NMP, and treated with 5×10^8 HLSC-EVs/g of liver; and WI+EV2 group ($n = 6$): livers exposed to 60 min of warm ischemia, perfused for 6 h with NMP, and treated with 25×10^8 HLSC-EVs/g of liver. The HLSC-EV treatment was administered via the NMP circuit within 15 min from perfusion start, as soon as hemodynamic parameters

were stable. In particular, the HLSC-EVs were suspended in 1 ml of saline and injected with a syringe directly into the circuit via a three-way stopcock placed upstream to the liver. In the NO INJURY and WI groups, an equivalent volume of saline alone was added.

Perfusate analysis and bile production

Perfusate samples were collected hourly to perform blood gas analyses (ABL 725 Radiometer, Copenhagen) and to measure ALT, AST, and phosphate levels (Biochemistry Laboratory, Molinette Hospital). Bile was collected through a PTFE tube and weighted.

Histopathology and fluorescence analyses

To analyze HLSC-EVs uptake and to evaluate liver histologic features and glycogen deposits, liver samples collected at the end of each experiment were processed and analyzed as described in Panel S2. In particular, two pathologists (AG and ED) independently assessed and graded tissue injury signs using the Suzuki score system [37]. Cellular proliferation was detected with proliferating cell nuclear antigen (PCNA) analysis [19].

RNA extraction and real-time polymerase chain reaction

RNA extraction and real-time polymerase chain reaction (RT-PCR) protocols are described in Table S1.

Protein extraction and western blot analysis

Protein extraction and Western blot (WB) analysis are described in Panel S3.

Statistical analysis

Data are presented as mean ± standard error of the mean (SEM). Statistical analyses were performed using one-way or two-way ANOVA or Kruskal–Wallis test, depending on data normality; post hoc tests were performed with Tukey's multiple comparison test or Dunn's multiple comparison test as appropriate (GraphPad Prism, version 6.00). A P value <0.05 was considered as statistically significant.

Results

Perfusion parameters were homogeneous in the study groups, and no differences were observed in terms of weight, oxygenation, hematocrit, and perfusion pressure (Table S2).

The presence of Dil-stained HLSC-EVs was observed with immunofluorescence analysis. In the WI+EV1 and WI+EV2 groups, it was possible to detect the presence of HLSC-EVs (in red) within the hepatic tissue (Fig. 1a).

Regarding the histopathological evaluation (Fig. 1b–d), Suzuki's score of the WI group showed a higher degree of necrosis than the NO INJURY group (2.17 ± 0.48 vs. 0.67 ± 0.21, $P = 0.037$). Similarly, less necrosis was observed in the WI+EV2 group if compared to the WI group (0.67 ± 0.33 vs. 2.17 ± 0.48, $P = 0.037$) (Fig. 1b and e). Glycogen deposits were distributed with a heterogeneous and azonal pattern, in both hepatocyte cytoplasms and sinusoids (Fig. 1c). The percentage of proliferating cells in the WI group tissues was low, with an average slightly above 1% and significantly inferior than the PCNA index of the NO INJURY group (1.49 ± 0.58 vs. 16.0 ± 4.27, $P = 0.027$). In the treated groups, the PCNA index was similar to that of the NO INJURY group, but only the WI+EV2 group reached a statistically significative difference when compared to the WI group (15.0 ± 6.66 vs. 1.49 ± 0.58, $P = 0.048$) (Fig. 1d and f).

Vascular resistance of the liver was calculated as the ratio between pressure and flow. At 6 h of perfusion, the livers from the NO INJURY group showed significantly lower resistance if compared to the WI group (1.66 ± 0.36 vs. 3.73 ± 0.96, $P < 0.0001$) and WI+EV1 group (1.66 ± 0.36 vs. 2.78 ± 0.47, $P = 0.038$). In the WI+EV2 group, a significant reduction in vascular resistance compared to the WI group was observed at 6 h (3.73 ± 0.96 vs. 2.48 ± 0.16, $P = 0.016$) (Fig. 2a).

Cumulative bile production was significantly higher in the NO INJURY group than in the WI and WI+EV1 groups at 3, 4, 5, and 6 h. Moreover, the livers from the WI+EV2 group produced twofold bile than the WI livers at 6 h of NMP (1961 ± 368 mg vs. 898.2 ± 496 mg, $P = 0.044$) (Fig. 2b).

A gradual increase in perfusate transaminase levels during NMP was observed in all the experimental groups (Fig. 2c and d). Compared to the NO INJURY controls, the livers from the WI group released significantly more ALT, from the 4th hour of perfusion, and AST, from the 3rd hour of perfusion. HLSC-EV treatment allowed a significant reduction of ALT at the end of perfusion, with significantly lower levels both in the WI+EV1 group and in the WI+EV2 group, compared to the WI group (13.42 ± 4.50 U/l/g of liver vs. 35.39 ± 10.5 U/l/g of liver, $P = 0.0008$ and 16.87 ± 4.02 U/l/g
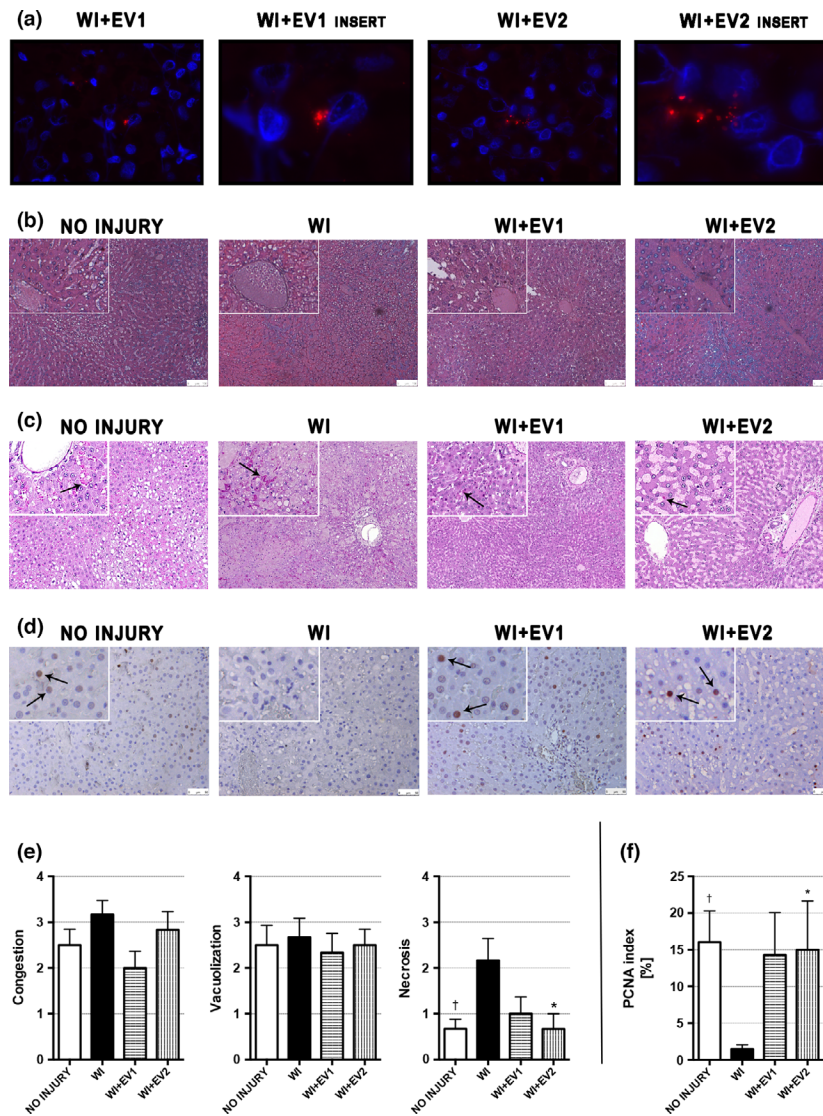
Figure 1 Histopathology and fluorescence analyses performed on perfused livers after 6 h of NMP. (a) Representative micrographs showing Hoechst-stained cell nuclei (blue) and Dil/Did-stained HLSC-EVs (red) (original magnification 630×, inserts at 2520×). (b) Representative micrographs of H&E stain (original magnification 200×, inserts at 400×, scale bar 100 μm). (c) Representative sections of glycogen distribution. PAS-positive glycogen deposits (black arrows) were observed in hepatocytes and sinusoids with no specific pattern nor parenchymal distribution throughout groups (original magnification 100×, inserts at 200×). (d) Representative micrographs of proliferating cell nuclear antigen (PCNA)-stained liver tissues (original magnification at 400×, inserts at 800×, scale bar 50 μm); the black arrows indicate representative PCNA-positive cells. (e) Quantitative scoring for liver tissue injury according to Suzuki's histologic criteria. [†]WI versus NO INJURY and *WI versus WI+EV2. Data are represented as mean ± SEM. (f) PCNA index obtained by blindly counting PCNA-positive and PCNA-negative cells on 10 HPF per each liver and expressed as the percentage of PCNA-positive cells on total cells. [†]WI versus NO INJURY and *WI versus WI+EV2. Data are represented as mean ± SEM.

of liver vs. 35.39 ± 10.5 U/l/g of liver, $P = 0.0069$, respectively) (Fig. 2c). Similarly, both doses of HLSC-EVs allowed a significant reduction in AST release compared to the WI group at 6 h of perfusion (51.06 ± 16.8 U/l/g of liver vs. 79.08 ± 12.1 U/l/g of liver, $P = 0.030$, and 49.31 ± 7.69 U/l/g of liver vs. 79.08 ± 12.1 U/l/g of liver, $P = 0.018$, respectively, for WI+EV1 and WI+EV2); in addition, compared to the

ischemic controls, the higher dose of HLSC-EVs was associated with lower levels of AST even at the 4th hour of perfusion (20.60 ± 3.21 U/l/g of liver vs. 48.35 ± 12.2 U/l/g of liver, $P = 0.033$) (Fig. 2d).

Bicarbonate was added where necessary to maintain perfusate pH above the minimum threshold (≥ 7.30) (Fig. 3a-c). In the NO INJURY, WI+EV1, and WI+EV2 groups, the livers were able to self-regulate the pH of
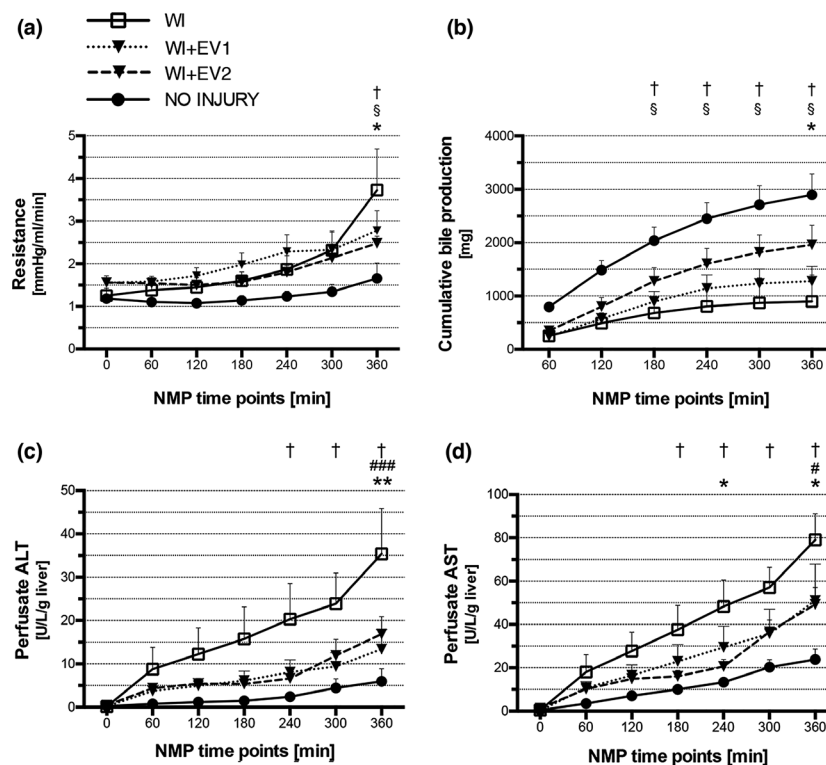
Figure 2 Liver resistance, bile production, and cytolysis during NMP. (a) Vascular resistance of the liver, expressed as the ratio between pressure and flow. [†]WI versus NO INJURY, [§]NO INJURY versus WI+EV1, and *WI versus WI+EV2. Data are represented as mean ± SEM. (b) Cumulative bile production. Each value represents total volume of bile produced from perfusion start to the relative time point. [†]WI versus NO INJURY, [§] NO INJURY versus WI+EV1, and *WI versus WI+EV2. Data are represented as mean ± SEM. (c) Perfusate alanine aminotransferase levels during 6 h of NMP. [†]WI versus NO INJURY, [#]WI versus WI+EV1, and *WI versus WI+EV2. Data are represented as mean ± SEM. (d) Perfusate aspartate aminotransferase levels during 6 h of NMP. [†]WI versus NO INJURY, [#]WI versus WI+EV1, and *WI versus WI+EV2. Data are represented as mean ± SEM.

the perfusate almost autonomously. By contrast, in the WI group the acid–base homeostasis was strongly compromised, with a tendency to acidosis. Thus, total administration of bicarbonate during perfusion was significantly higher in the WI group compared to the NO INJURY group (4.00 ± 0.37 mEq vs. 1.33 ± 0.42 mEq, $P = 0.0006$), to the WI+EV1 group (4.00 ± 0.37 mEq vs. 1.00 ± 0.26 mEq, $P = 0.0002$), and to the WI+EV2 group (4.00 ± 0.37 mEq vs. 1.33 ± 0.49 mEq, $P = 0.0006$) (Fig. 3a). In particular, the livers from the WI group received higher amounts of HCO_3^- than those from the WI+EV1 group and the WI+EV2 group after 3 h (0.83 ± 0.17 mEq vs. 0.00 ± 0.00 mEq, $P = 0.0009$, and 0.83 ± 0.17 mEq vs. 0.17 ± 0.17 mEq, $P = 0.012$) and after 4 h (0.67 ± 0.21 mEq vs. 0.17 ± 0.17 mEq, $P = 0.0009$, and 0.67 ± 0.21 mEq vs. 0.33 ± 0.21 mEq, $P = 0.012$) (Fig. 3b). Interestingly, a significant difference between the WI group and the WI+EV2 group was already seen after 2 h of NMP (0.83 ± 0.17 mEq vs. 0.17 ± 0.17 mEq, $P = 0.012$).

Phosphate perfusate levels were significantly higher in the WI group compared to the NO INJURY group at all time points. In the WI+EV2 group, significantly lower phosphate levels were observed compared to the WI group at 3 and 4 h of NMP (0.185 ± 0.03 mg/dl/g of liver vs. 0.295 ± 0.03 mg/dl/g of liver, $P = 0.012$, and 0.170 ± 0.03 mg/dl/g of liver vs. 0.303 ± 0.02 mg/dl/g of liver, $P = 0.001$, respectively), while the lower dose allowed a significant reduction of phosphates compared to the WI group only at 4 h (0.192 ± 0.03 mg/dl/g of liver vs. 0.303 ± 0.02 mg/dl/g of liver, $P = 0.010$) (Fig. 3d).

We analyzed the relative expression of several genes, involved in different pathways: inflammation (CXCL-10, IL-6, TLR-4); immune response (NF-kB, CD14); oxidative stress (SOD1, eNOS); apoptosis (BAX, BCL-2); endothelial cells response (ICAM1, VCAM1, P-Selectin, E-selectin); and autophagy (Beclin-1, mTOR, ULK1). RT-PCR results did not show any significant changes between the four experimental groups (Fig. S3).
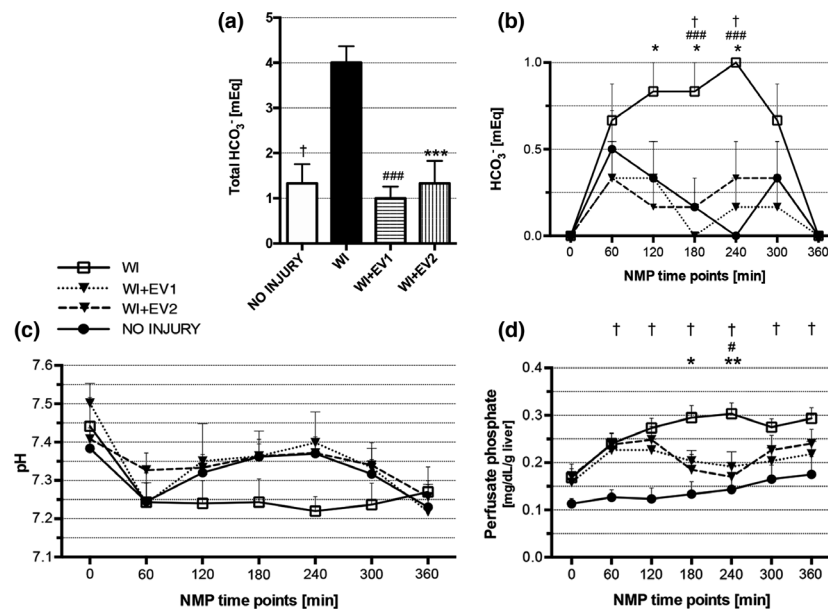
Figure 3 Metabolic parameters during NMP. (a) Sum of total mEq of HCO_3^- added to the perfusate during 6 h of NMP. [†]WI versus NO INJURY, [#]WI versus WI+EV1, and *WI versus WI+EV2. Data are represented as mean ± SEM. (b) mEq of HCO_3^- added to the perfusate at each time point of NMP. [†]WI versus NO INJURY, [#]WI versus WI+EV1, and *WI versus WI+EV2. Data are represented as mean ± SEM. (C) Perfusate pH during 6 h of NMP. Data are represented as mean ± SEM. (d) Perfusate phosphate levels during 6 h of NMP. [†]WI versus NO INJURY, [#]WI versus WI+EV1, and *WI versus WI+EV2. Data are represented as mean ± SEM.

Finally, we analyzed the endothelial cell response at the protein level by WB analysis: No significant differences were observed among the study groups (Fig. S4).

Discussion

The use of DCD in LT has reached acceptable overall outcomes if warm ischemia is kept short (<30 min) [38,39], whereas restrictive inclusion criteria are applied to DCD grafts with prolonged warm ischemia, resulting in high discard rates [40]. NMP is an innovative technique for liver preservation, especially when used with ECD organs [10,41–43]. This method keeps the graft metabolically active, allowing to assess the organ quality, and gives the opportunity to pharmacologically treat the livers with the aim of further improving sub-optimal organs [14,15]. In particular, NMP has recently become a promising candidate for stem cell and stem cell-derived therapies, as it offers the possibility to monitor their liver-specific delivery and to maximize their therapeutic activity [16,27,28,44].

HLSCs are stem cells resident in the hepatic parenchyma with regenerative and hepatoprotective properties [18,19]. Products derived from HLSCs, such as conditioned medium and HLSC-EVs, are able to mimic most of the effects of HLSCs, including mitogenic activity

and apoptosis inhibition, through the transfer of proteins, mRNA, and miRNA [21,45].

Recently, in a 4-hour hypoxic NMP model, we demonstrated the possibility of treating rat livers with HLSC-EVs [27]. On this basis, we decided to evaluate the efficacy of HLSC-EVs in a 6-hour NMP model that mimics a high-risk DCD condition. In the present study, we included four experimental groups: one group representative of a standard donation with no ischemic damage and three groups consisting of organs exposed to a prolonged period (60 min) of warm ischemia. In two of the three high-risk DCD groups, HLSC-EVs were administered at two different dosages to assess the treatment efficacy in reducing IRI and to identify a possible dose–effect correlation.

The ability of HLSC-EVs to localize into the hepatic tissue is an integrin-mediated mechanism [21]. In the present study, the uptake of HLSC-EVs by the liver was further confirmed, as shown by epifluorescence microscopy images.

Histopathological analysis was performed on H&E-stained tissues using a specific score for IRI [37]. Ischemia caused a crucial damage on liver tissue, as demonstrated by the presence of diffuse necrotizing in the WI group. Interestingly, a higher dose of HLSC-EVs only was able to limit ischemic injury significantly. The

PCNA analysis evidenced the presence of actively proliferating cells both in the NO INJURY group and in the treated groups, in a percentage close to 15% of the total cells. By contrast, in the WI group, cell proliferation was almost absent. Again, significantly higher proliferation rates were observed in the WI+EV2 group when compared to the WI group. Altogether, these data confirmed previous evidence on the ability of HLSC-EVs to reduce the extension of necrosis and to maintain liver regeneration [21,27].

Hemodynamic parameters are among the criteria proposed to assess liver viability during NMP [46]. In all the experimental groups, a progressive increase in resistance over time was observed, particularly evident in the groups subjected to the ischemic damage. The higher dose of HLSC-EVs was able to significantly reduce the intrahepatic resistance compared to the WI controls. The ability of NMP to improve graft hemodynamics performance has already been described [34]. However, in our study, only the association between NMP and HLSC-EVs at the higher dose was effective and these results were consistent with histology.

Bile production and pH self-regulation are two important indicators of liver metabolic activity during NMP [10,47]. Both HLSC-EV doses were able to reduce the total need of bicarbonate during perfusion; more specifically, while the ischemic livers were constantly added with HCO^{3-} from the first hour of NMP, the treated livers tended to self-regulate the acid–base homeostasis with progressive increasing pH values and decreasing need of bicarbonate. pH regulation was particularly efficient in the WI+EV2 group, that, as a consequence, received significantly less bicarbonate than the WI group from the 2nd to the 4th hour of perfusion. Cumulative bile production was significantly increased only in the WI+EV2 group, while in the WI+EV1 group we observed a not significant increasing trend. Bile acids are mainly synthesized by zone 1 and zone 2 hepatocytes, while HCO_3^- is produced in the zone 3 [48]. Moreover, liver acid–base regulation depends strictly on its metabolic activity and, in particular, on the pH-dependent glutaminases localized in zone 1 [49]. Hence, these data suggest that HLSC-EVs protected the whole hepatic lobule from IRI and increased the metabolic activity of the liver in a dose-dependent manner.

In the NMP setting, perfusate ALT levels are often considered as direct indicators of organ viability [36], while the post-LT AST peak, a surrogate marker of graft survival, is commonly used as a major outcome in clinical trials involving NMP [9]. In the present study, the livers from the NO INJURY group released low levels of transaminases in the perfusate, whereas in the WI group ALT and AST curves are particularly steep and significantly higher if compared to healthy controls. Both dosages of HLSC-EVs allowed a significant reduction in ALT and AST levels at 6 h of perfusion compared to ischemic controls. In addition, the higher dose of HLSC-EVs was able to anticipate the effect of the treatment, as confirmed by lower levels of AST values at 4 h. These data confirmed our previous evidence [27,29] and demonstrated the ability of HLSC-EVs to reduce cytolysis during perfusion with NMP.

Serum phosphate levels are a clinical parameter that correlates with the prognosis of patients suffering from fulminant hepatitis [50]. In particular, phosphate is a fundamental substrate for mitochondrial ATP synthesis, and therefore, an increase in its concentration may indicate a decreased oxidative phosphorylation. ATP depletion plays a key role during IRI, and, in fact, in the WI group, phosphate levels were significantly higher compared to healthy controls at every time point. On the other hand, hypophosphatemia is commonly observed after hepatic resection. Despite its predictive role in the development of postoperative complications is still controversial, it is likely that a drop in serum phosphate may potentially indicate an efficient liver regeneration [51,52]. In our model, an inversion toward phosphate levels was observed in treated groups between the third and fourth hour of perfusion and this may suggest that HLSC-EVs were able to promote the recovery of ATP synthesis and hepatocellular cell growth. This hypothesis would be consistent with PCNA findings, confirming the active role of HLSC-EVs in promoting hepatocyte proliferation [21].

In conclusion, this study demonstrates that HLSC-EV treatment is an effective option to recondition ischemic livers during NMP. Between the two administered doses, the higher one allowed better results in all the study outcomes. Nonetheless, these preliminary findings must be interpreted considering some limitations. First, we did not observe significant differences in the RNA levels of the targets evaluated in this study, despite our previous experience on several pathways modulated by HLSCs in different models of liver injury [29,53,54]. On the basis of some trends observed in the expression of genes related to endothelial cell activation (VCAM-1, P-Selectin, and E-Selectin), we investigated their expression also at the protein level but again there were no significant changes among the study groups. One possible explanation could be that HLSC-EVs exert their effects quite early, as described in our previous NMP study [27], and thus, biopsies, taken after 6 h of ex vivo NMP, may have been performed too late to observe significant changes at a molecular level. Of note, the most relevant effects of HLSC-EVs were observed between the 3rd and the 4th

hour of NMP, while from the 5th hour of perfusion, a trend toward a worsened liver function was observed in all the study groups, even in the NO INJURY one. It is conceivable that our NMP circuit was not completely effective in preserving livers after 4 h, and thus, some of the beneficial effects of HLSC-EVs on histology and gene expression might have been lost during the last 2 h of perfusion. Moreover, transplantation of machine-perfused livers was not performed in our experimental model since little was known about the effects of HLSC-EV and their appropriate administration doses in the NMP setting. Thus, the potential impact of HLSC-EVs on post-transplant outcomes still needs to be evaluated. To add knowledge to this promising reconditioning protocol, further investigations including different ECD conditions with shorter perfusion time and, finally, with an in vivo reperfusion model are warranted.

Authorship

NDS and VNT contributed equally to this work. NDS, VNT, DR, AC and FR performed the experimental procedures, collected and analyzed the data, and wrote and revised the manuscript. ED and AG contributed in histopathological analyses. DB provided important experimental materials. AA, DP, GC and RR designed the study, analyzed the data, and revised the manuscript.

Funding

Conflict of interest

GC was a component of the scientific advisory board of Unicyte AG. VNT and GC were named inventors in related patents. The remaining authors declare that the research was conducted in the absence of any commercial or financial relationships that could be construed as a potential conflict of interest.

Acknowledgements

SUPPORTING INFORMATION

Additional supporting information may be found online in the Supporting Information section at the end of the article.

Figure S1. Cytofluorimetric characterization of HLSC-EV by multiplex bead-based flow cytometry assay.

Figure S2. Methods for surgical procedure and liver procurement.

Figure S3. RT-PCR relative quantification mean (RQ mean) of RNA expression after 6 h of ex vivo NMP.

Figure S4. Protein levels measured by Western blot analysis of VCAM-1, P-Selectin and E-Selectin.

Table S1. RNA extraction and RT-PCR methods and primers list.

Table S2. Liver weight and operating parameters during NMP.

Panel S1. Methods for HLSC isolation and culture.

Panel S2. Methods for histopathology and fluorescence analyses.

Panel S3. Methods for protein extraction and Western blot analysis.

REFERENCES

1. Hodgson R, Young AL, Attia MA, Lodge JPA. Impact of a national controlled donation after circulatory death (DCD) program on organ donation in the United Kingdom: a 10-year study. *Am J Transplant* 2017; **17**: 3172.

2. O'Neill S, Roebuck A, Khoo E, Wigmore SJ, Harrison EM. A meta-analysis and meta-regression of outcomes including biliary complications in donation after cardiac death liver transplantation. *Transpl Int* 2014; **27**: 1159

3. Briceño J, Marchal T, Padillo J, Solòrzano G, Pera C. Influence of marginal donors on liver preservation injury. *Transplantation* 2003; **74**: 522

4. Laing RW, Scalera I, Isaac J, *et al.* Liver transplantation using grafts from donors after circulatory death: a propensity score-matched study from a single center. *Am J Transplant* 2016; **16**: 1795.

5. Schlegel A, Muller X, Dutkowski P. Machine perfusion strategies in liver transplantation. *HepatoBiliary Surg Nutr* 2019; **8**: 490.

6. Lee DD, Singh A, Burns JM, Perry DK, Nguyen JH, Taner CB. Early allograft dysfunction in liver transplantation with donation after cardiac death donors results in inferior survival. *Liver Transplant* 2014; **20**: 1447.

7. Konishi T, Lentsch AB. Hepatic ischemia/reperfusion: mechanisms of tissue

injury, repair, and regeneration. *Gene Expr* 2017; **17**: 277.

8. Ravikumar R, Leuvenink H, Friend PJ. Normothermic liver preservation: a new paradigm? *Transpl Int* 2015; **28**: 690.

9. Nasralla D, Coussios CC, Mergental H, et al. A randomized trial of normothermic preservation in liver transplantation. *Nature* 2018; **557**: 50.

10. Ravikumar R, Jassem W, Mergental H, et al. Liver transplantation after ex vivo normothermic machine preservation: a phase 1 (first-in-man) clinical trial. *Am J Transplant* 2016; **16**: 1779.

11. Sharma AK, Laubach VE. Protecting donor livers during normothermic machine perfusion with stem cell extracellular vesicles. *Transplantation* 2018; **102**: 725.

12. Goldaracena N, Spetzler VN, Echeverri J, et al. Inducing hepatitis C virus resistance after pig liver transplantation—a proof of concept of liver graft modification using warm ex vivo perfusion. *Am J Transplant* 2017; **17**: 970.

13. Boteon YL, Attard J, Boteon APCS, et al. Manipulation of lipid metabolism during normothermic machine perfusion: effect of defatting therapies on donor liver functional recovery. *Liver Transplant* 2019; **25**: 1007.

14. Xu J, Buchwald JE, Martins PN. Review of current machine perfusion therapeutics for organ preservation. *Transplantation* 2020; **104**: 1792.

15. Dengu F, Abbas SH, Ebeling G, Nasralla D. Normothermic machine perfusion (NMP) of the liver as a platform for therapeutic interventions during ex-vivo liver preservation: a review. *J Clin Med* 2020; **9**: 1046.

16. Laing RW, Stubblefield S, Wallace L, et al. The delivery of multipotent adult progenitor cells to extended criteria human donor livers using normothermic machine perfusion. *Front Immunol* 2020; **11**: 1.

17. Thompson ER, Connelly C, Ali S, Sheerin NS, Wilson CH. Cell therapy during machine perfusion. *Transpl Int* 2021; **34**: 49.

18. Herrera MB, Bruno S, Buttiglieri S, et al. Isolation and characterization of a stem cell population from adult human liver. *Stem Cells* 2006; **24**: 2840.

19. Herrera MB, Fonsato V, Bruno S, et al. Human liver stem cells improve liver injury in a model of fulminant liver failure. *Hepatology* 2013; **57**: 311.

20. Navarro-Tableros V, Herrera Sanchez MB, Figliolini F, Romagnoli R, Tetta C, Camussi G. Recellularization of rat liver scaffolds by human liver stem cells. *Tissue Eng Part A* 2015; **21**: 1929.

21. Herrera MB, Fonsato V, Gatti S, et al. Human liver stem cell-derived microvesicles accelerate hepatic regeneration in hepatectomized rats. *J Cell Mol Med* 2010; **14**: 1605.

22. Sanchez M, Bruno S, Grange C, et al. Human liver stem cells and derived extracellular vesicles improve recovery in a murine model of acute kidney injury. *Stem Cell Res Ther* 2014; **5**: 124.

23. Kholia S, Herrera Sanchez MB, Cedrino M, et al. Human liver stem cell-derived extracellular vesicles prevent aristolochic acid-induced kidney fibrosis. *Front Immunol* 2018; **9**: 1639.

24. Herrera MB, Previdi S, Bruno S, et al. Extracellular vesicles from human liver stem cells restore argininosuccinate synthase deficiency. *Stem Cell Res Ther* 2017; **8**: 1.

25. Quesenberry PJ, Aliotta J, Deregibus MC, Camussi G. Role of extracellular RNA-carrying vesicles in cell differentiation and reprogramming. *Stem Cell Res Ther* 2015; **6**: 1.

26. Grange C, Bellucci L, Bussolati B, Ranghino A. Potential applications of extracellular vesicles in solid organ transplantation. *Cells* 2020; **9**: 1.

27. Rigo F, De Stefano N, Navarro-Tableros V, et al. Extracellular vesicles from human liver stem cells reduce injury in an ex vivo normothermic hypoxic rat liver perfusion model. *Transplantation* 2018; **102**: e205.

28. Rigo F, Navarro-Tableros V, De Stefano N, Calleri A, Romagnoli R. Ex vivo normothermic hypoxic rat liver perfusion model: an experimental setting for organ recondition and pharmacological intervention. *Methods Mol Biol* 2021; **139**.

29. Calleri A, Roggio D, Navarro-Tableros V, et al. Protective effects of human liver stem cell-derived extracellular vesicles in a mouse model of hepatic ischemia-reperfusion injury. *Stem Cell Rev Reports* 2021; **17**: 459.

30. Grange C, Tapparo M, Bruno S, et al. Biodistribution of mesenchymal stem cell-derived extracellular vesicles in a model of acute kidney injury monitored by optical imaging. *Int J Mol Med* 2014; **33**: 1055.

31. Bruno S, Grange C, Collino F, et al. Microvesicles derived from mesenchymal stem cells enhance survival in a lethal model of acute kidney injury. *PLoS One* 2012; **7**: e33115.

32. op den Dries S, Karimian N, Westerkamp AC, et al. Normothermic machine perfusion reduces bile duct injury and improves biliary epithelial function in rat donor livers. *Liver Transplant* 2016; **22**: 994.

33. Bessems M, 't Hart NA, Tolba R, et al. The isolated perfused rat liver: standardization of a time-honoured model. *Lab Anim* 2006; **40**: 236.

34. Izamis M-L, Calhoun C, Uygun BE, et al. Simple machine perfusion significantly enhances hepatocyte yields of ischemic and fresh rat livers. *Cell Med* 2013; **4**: 109.

35. Berendsen TA, Bruinsma BG, Lee J, et al. A simplified subnormothermic machine perfusion system restores ischemically damaged liver grafts in a rat model of orthotopic liver transplantation. *Transplant Res* 2012; **1**: 1.

36. Uygun K, Tolboom H, Izamis ML, et al. Diluted blood reperfusion as a model for transplantation of ischemic rat livers: Alanine aminotransferase is a direct indicator of viability. *Transplant Proc* 2010; **42**: 2463.

37. Suzuki S, Toledo-Pereyra LH, Rodriguez FJ, Cejalvo D. Neutrophil infiltration as an important factor in liver ischemia and reperfusion injury. Modulating effects of FK506 and cyclosporine. *Transplantation* 1993; **55**: 1265.

38. Croome KP, Lee DD, Perry DK, et al. Comparison of longterm outcomes and quality of life in recipients of donation after cardiac death liver grafts with a propensity-matched cohort. *Liver Transplant* 2017; **23**: 342.

39. Schlegel A, Kalisvaart M, Scalera I, et al. The UK DCD risk score: a new proposal to define futility in donation-after-circulatory-death liver transplantation. *J Hepatol* 2018; **68**: 456.

40. Manyalich M, Nelson H, Delmonico FL. The need and opportunity for donation after circulatory death worldwide. *Curr Opin Organ Transplant* 2018; **23**: 136.

41. Imber CJ, St. Peter SD, Lopez de Cenarruzabeitia I, et al. Advantages of normothermic perfusion over cold storage in liver preservation. *Transplantation* 2002; **73**: 701.

42. St Peter SD, Imber CJ, Lopez I, Hughes D, Friend PJ. Extended preservation of non-heart-beating donor livers with normothermic machine perfusion. *Br J Surg* 2002; **89**: 609.

43. Brockmann J, Reddy S, Coussios C, et al. Normothermic perfusion: a new paradigm for organ preservation. *Ann Surg* 2009; **250**: 1.

44. Carlson K, Kink J, Hematti P, Al-Adra DP. Extracellular vesicles as a novel therapeutic option in liver transplantation. *Liver Transplant* 2020; **26**: 1522.

45. Camussi G, Deregibus MC, Cantaluppi V. Role of stem-cell-derived microvesicles in the paracrine action of stem cells. *Biochem Soc Trans* 2013; **41**: 283.

46. Mergental H, Perera MTPR, Laing RW, et al. Transplantation of declined liver allografts following normothermic ex-situ evaluation. *Am J Transplant* 2016; **16**: 3635.

47. Watson CJE, Kosmoliaptsis V, Randle LV, et al. Normothermic perfusion in the assessment and preservation of declined livers before transplantation: hyperoxia and vasoplegia-important lessons from the first 12 cases. *Transplantation* 2017; **101**: 1084.

48. Gebhardt R. Metabolic zonation of the liver: regulation and implications for liver function. *Pharmacol Ther* 1992; **53**: 275.

49. Watson CJE, Jochmans I. From, "Gut Feeling" to objectivity: machine preservation of the liver as a tool to assess organ viability. *Curr Transplant Reports* 2018; **5**: 72.

50. Chung PY, Sitrin MD, Te HS. Serum phosphorus levels predict clinical outcome in fulminant hepatic failure. *Liver Transplant* 2003; **9**: 248.

51. Hallet J, Karanicolas PJ, Zih FSW, et al. Hypophosphatemia and recovery of post-hepatectomy liver insufficiency. *HepatoBiliary Surg Nutr* 2016; **5**: 217.

52. Warner SG, Jutric Z, Nisimova L, Fong Y. Early recovery pathway for hepatectomy: data-driven liver resection care and recovery. *HepatoBiliary Surg Nutr* 2017; **6**: 297.

53. Bruno S, Pasquino C, Herrera Sanchez MB, et al. HLSC-derived extracellular vesicles attenuate liver fibrosis and inflammation in a murine model of non-alcoholic steatohepatitis. *Mol Ther* 2020; **28**: 479.

54. Chiabotto G, Pasquino C, Camussi G, Bruno S. Molecular pathways modulated by mesenchymal stromal cells and their extracellular vesicles in experimental models of liver fibrosis. *Front Cell Dev Biol* 2020; **8**: 1.